

Evaluation of Assumptions in Foot and Ankle Biomechanical Models

Authors:

- Hamed Malakoutikhah¹, PhD, hamedmalak@arizona.edu

- Cesar de Cesar Netto², MD, PhD, Assistant Professor, cesar-netto@uiowa.edu

- Erdogan Madenci¹, PhD, Professor, madenci@arizona.edu

- L. Daniel Latt³, MD, PhD, Associate Professor, dlatt@arizona.edu

Affiliations:

1. Department of Aerospace and Mechanical Engineering, University of Arizona, Tucson, AZ, USA

2. Department of Orthopaedics and Rehabilitation, University of Iowa, Iowa City, Iowa, USA

3. Department of Orthopaedic Surgery, University of Arizona, Tucson, AZ, USA

Corresponding Author:

Hamed Malakoutikhah (email address: hamedmalak@arizona.edu)

Address: 1130 N Mountain Ave, Tucson, AZ 85721, USA

Declarations of competing interest:

None

Funding:

None

Word count:

25 Main text excluding figure legends and references (4196 words), abstract (249 words)

26

27

28 **ABSTRACT**

29 *Background:* A variety of biomechanical models have been used in studies of foot and ankle disorders.

30 Assumptions about the element types, material properties, and loading and boundary conditions are

31 inherent in every model. It was hypothesized that the choice of these modeling assumptions could have a

32 significant impact on the findings of the model.

33 *Methods:* We investigated the assumptions made in a number of biomechanical models of the foot and

34 ankle and evaluated their effects on the results of the studies. Specifically, we focused on: (1) element

35 choice for simulation of ligaments and tendons, (2) material properties of ligaments, cortical and

36 trabecular bones, and encapsulating soft tissue, (3) loading and boundary conditions of the tibia,

37 fibula, tendons, and ground support.

38 *Findings:* Our principal findings are: (1) the use of isotropic solid elements to model ligaments and

39 tendons is not appropriate because it allows them to transmit unrealistic bending and twisting moments

40 and compressive forces; (2) ignoring the difference in elastic modulus between cortical and trabecular

41 bones creates non-physiological stress distribution in the bones; (3) over-constraining tibial motion

42 prevents anticipated deformity within the foot when simulating foot deformities, such as progressive

43 collapsing foot deformity; (4) neglecting the Achilles tendon force affects almost all kinetic and

44 kinematic parameters through the foot; (5) the axial force applied to the tibia and fibula is not equal to

45 the ground reaction force due to the presence of tendon forces.

46 *Interpretation:* The predicted outcomes of a foot model are highly sensitive to the model assumptions.

47

48 **Keywords:**

49 finite element analysis; computational and cadaveric models; material properties; loading and boundary
50 conditions; element types; adult acquired flatfoot deformity

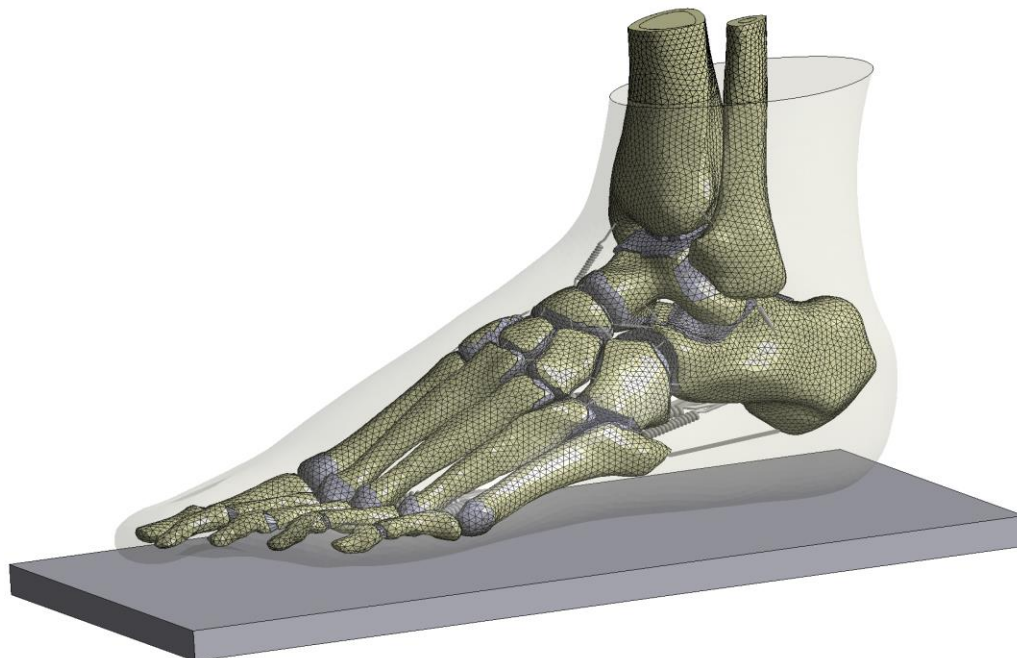
51

52 **1. INTRODUCTION**

53 Biomechanical models have been widely used to better understand the biomechanics and
54 pathomechanics of the human foot and to evaluate the effectiveness of surgical interventions. These
55 models differ significantly in terms of assumptions regarding the selection of element types and material
56 properties, the application of loading and boundary conditions, and the simulation of various foot
57 disorders (Morales-Orcajo et al., 2016; Wang et al., 2016; Behforootan et al., 2017). Specifically,
58 different element types with different characteristics, such as solid, shell, beam, truss, and spring
59 elements, have been used in computational studies to simulate the specific characteristics of different
60 tissues. Foot tissues have been modeled using a variety of material behaviors, including linear elasticity,
61 hyperelasticity, and viscoelasticity. In addition to element types and material properties, loading and
62 boundary conditions are other fundamental parameters that must be chosen in developing a model. The
63 choice of assumptions regarding the boundary conditions becomes especially important when simulating
64 foot deformities. For example, it is crucial to allow for external and internal rotation of the tibia when
65 modeling pes planus or pes cavus. To apply tendon forces and body weight (BW), a variety of
66 assumptions have been made in terms of loading locations and values. However, the variations that exist
67 in these assumptions may yield different results (Wang et al., 2016), raising concerns about the utility of
68 such models for medical decision-making. This is especially true in the case of boundary conditions,
69 where even minor variations in the constraints imposed on the degrees of freedom of tissues result in
70 markedly different biomechanical outcomes (Akrami et al., 2018; Hao et al., 2011; Altai et al., 2019; Hu
71 et al., 2017). Moreover, oversimplifications and questionable assumptions can cast doubt on the
72 predictions of a model. Understanding widely used modeling assumptions and their impact on model

73 outcomes will help improve future modeling efforts. Thus, the goal of this study was to examine the
74 contrasting approaches and assumptions that are commonly used in the development of foot models.
75 In each of the following sections, we first described the approaches used and the assumptions made in
76 defining modeling parameters, including (1) element types, (2) material properties, and (3) loading and
77 boundary conditions. Specifically, we described different element types used to model ligaments and
78 tendons; various material properties used to model ligaments, encapsulating soft tissue (EST) and
79 cortical and trabecular bones; and different loading conditions applied to the tibia and Achilles tendon.
80 We then evaluated their impacts on the results of the studies. The evaluation was done based on the
81 fundamental principles of mechanics such as force equilibrium conditions, force-deformation, and
82 stress-strain relationships, as well as material behavior under different loading conditions. We also
83 compared the results of different approaches, when needed, using a recently validated finite element
84 model of the foot reconstructed from CT scan images of a female cadaveric foot weighing 60 kg (Figure
85 1) (Malakoutikhah et al., 2022a). See Malakoutikhah et al. (2022a) for further details.

86



87

88

Figure 1. The finite element model of the foot used in this study

89

90 **2.1. Element types**

91 **2.1.1. Element choice for simulation of ligaments**

92 Tendons and ligaments have very small bending and compressive stiffness (Benjamin and Ralphs,
93 1998). To avoid transmitting moments and compressive forces, most studies have modeled ligaments as
94 tension-only spring or truss elements. In contrast, a few studies have modeled ligaments using isotropic
95 solid elements which are capable of transmitting bending and twisting moments as well as compressive
96 forces which real ligaments are unable to do. Although the distribution of resulting stress in axially
97 loaded members should be uniform, the predicted stress distribution across the cross sections of
98 ligaments and along the length of ligaments with constant cross-sectional area in these studies shows
99 large variations (Cifuentes-De la Portilla et al., 2019).

100 On the other hand, there are some situations in which pure tensile elements (springs and trusses) do
101 not adequately model ligament behavior because a portion of the loads is transmitted to the ligament by
102 direct contact with the ligament away from its attachment site on the bone. An example of this is the
103 spring ligament, which acts as a hammock, supporting the talar head and bearing a portion of the load
104 along the medial column. The inability to bear such lateral contact loads is a major limitation of axially
105 loaded members such as truss and spring elements. Therefore, there is a need to develop a 3D
106 anisotropic solid tension-only element capable of reflecting the tension-only characteristics of ligaments
107 that would be more suitable to account for the loads through soft tissue contact.

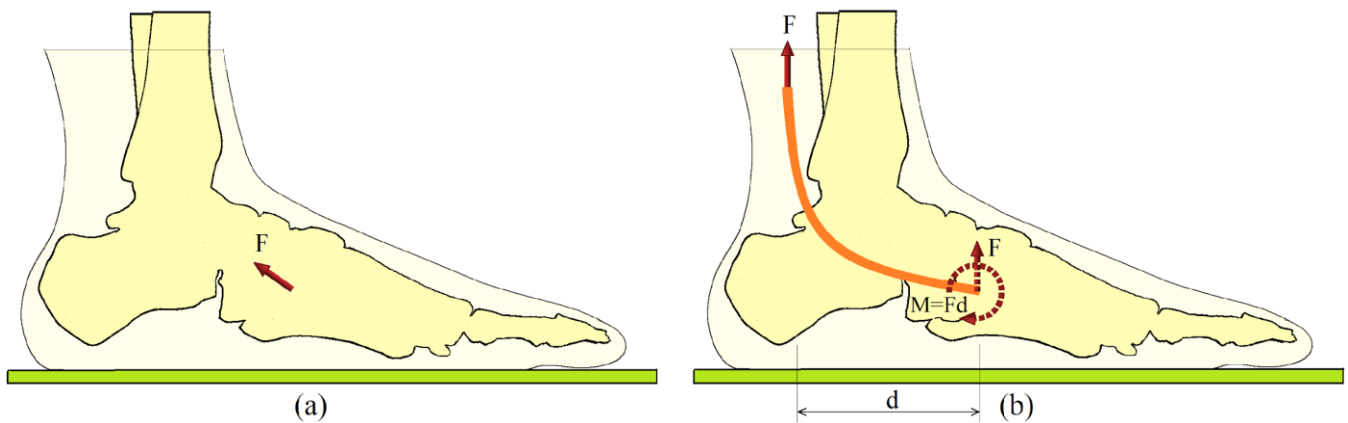
108

109 **2.1.2. Element choice for simulation of tendons**

110 Almost all computational models simulate the tendon forces through the use of force vectors. In most of
111 these models, the force vectors are applied at tendon insertion points on the bones along the tendon line
112 of action (Figure 2a). On the other hand, tendon force vectors are applied at the free end of tendons

113 (Figure 2b) in the foot models with isotropic solid elements representing tendons. However, an
114 unrealistic moment (M) develops along with the force at the tendon insertion points on the bone (Figure
115 2b) when a curved tendon with high bending stiffness is loaded; this alters the load distribution through
116 the foot. Moreover, unrealistic stresses induced in any given section of the tendon limit the predictive
117 capability of these models for examining stress patterns through the tendon.

118



119

120 **Figure 2.** a) Tendon force is applied to tendon insertion points along the tendon line of action, b) tendon
121 force is applied at the free end of the tendon modeled with isotropic solid elements

122

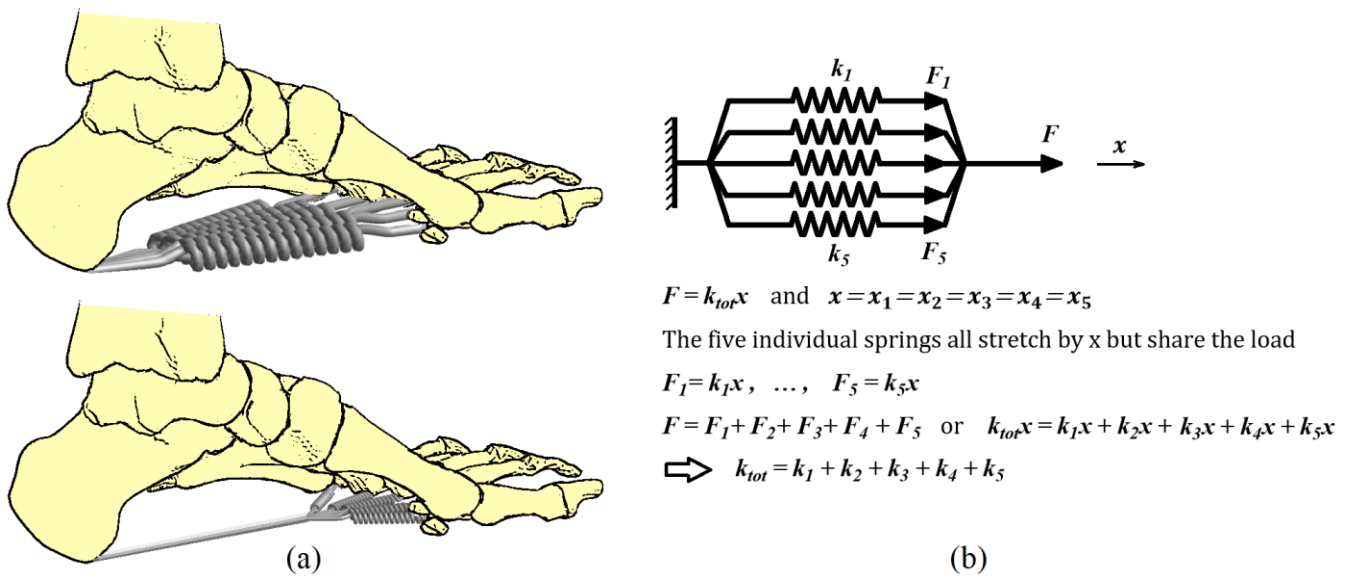
123 2.2. Material properties

124 2.2.1. Stiffness of ligaments with multiple bands

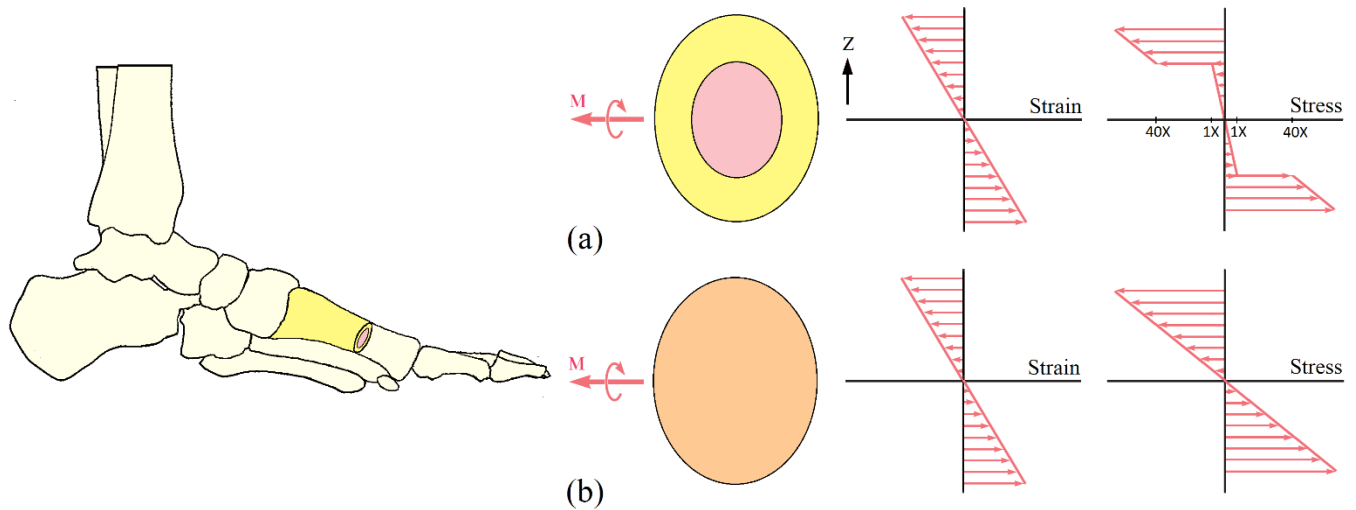
125 The stiffness of the plantar fascia and long plantar ligament is typically derived from published
126 cadaveric testing. For instance, a cadaveric study (Kitaoka et al., 1994) reported an overall stiffness of
127 203.2 N/mm for the plantar fascia. This value was determined by mounting the fascia specimens in a
128 tensile testing machine. The central band of plantar fascia originates on the calcaneal tuberosity and
129 extends distally, splitting into five bands which insert on the plantar plates of the five toes. Therefore,
130 the plantar fascia can be modeled as five separate bundles (Figure 3a) with specific axial stiffness in
131 computational studies. The axial stiffness ($k = AE/L$) facilitates the assignment of geometry (cross-

132 sectional area A and length L) and material properties (elastic modulus E) to ligaments. Some studies
 133 assigned the overall stiffness of 203.2 N/mm to each bundle. However, the sum of the stiffness of the
 134 bundles to all five rays should be equal to the plantar fascia's overall stiffness of 203.2 N/mm because
 135 they are connected in parallel (Figure 3b). Thus, the stiffness of each bundle is a fraction of the total
 136 stiffness, which can be assumed to be $203.2/5 = 40.6$ N/mm. Given that the medial and middle zones of
 137 the plantar fascia are stiffer than the lateral zone (Kitaoka et al., 1994), assigning 60 N/mm to the first
 138 branch, 40 N/mm to the second and third, and 30 N/mm to the fourth and fifth may provide a more
 139 precise prediction. This is also true for the long plantar ligament, which is divided into four distinct
 140 bands distally. This misinterpretation of stiffness directly affects the elongation and strain of these
 141 primary stabilizers of the foot, as well as the overall configuration of the foot.

142



149 Despite the significant difference in elastic modulus between cortical and trabecular bones (14000 MPa
 150 vs 350 MPa) (Siegler et al., 1988), some computational studies assign them the same material properties,
 151 often the average of the two. This simplification has a negligible effect on the foot alignment because of
 152 the high stiffness and consequently very small deformation of bones under working conditions.
 153 However, this simplification has a negative impact on the outcomes when it comes to evaluating the
 154 stress distribution in the bones. According to classical elasticity, there is no discontinuity in strain at the
 155 interface between trabecular and cortical bones since the displacement at the interface is continuous
 156 (Figure 4a). On the other hand, strain continuity necessitates stress discontinuity at the interfaces due to
 157 the difference in the elastic modulus of the two materials (Figure 4a). However, if the same material is
 158 assigned to the cortical and trabecular bones, the stress will be incorrectly distributed (Figure 4b).
 159



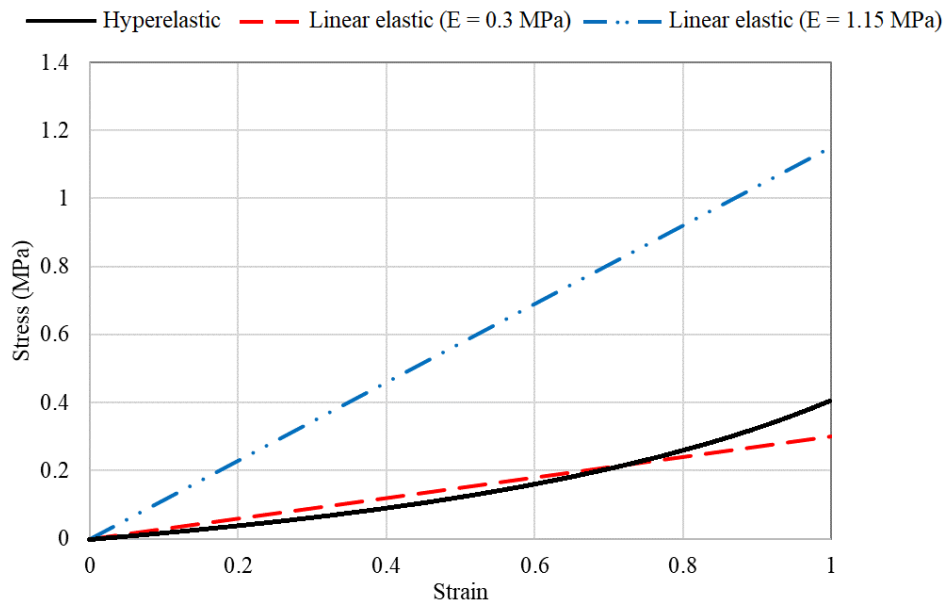
160
 161 **Figure 4.** The distribution of strain and stress in a section of the first metatarsal bone subjected to
 162 bending moment for the cortical and trabecular bones with a) different elastic moduli, b) the same elastic
 163 modulus (the average of both)

164

165 **2.2.3. Material properties of the EST**

166 Some computational models of the foot include an EST to better simulate entire anatomical structure of
167 the foot, loading conditions on the sole of the foot, and the frictional interface with the floor. The
168 presence of the EST also facilitates the convergence of the model by providing cushioning to the
169 underlying bones and shock absorption between the contact surfaces. The EST is subjected to large
170 deformations due to its low stiffness. The linear elastic material with an elastic modulus of $E = 0.3$ (Hsu
171 et al., 2005) and $E = 1.15$ MPa (Chu et al., 1995), as well as the hyperelastic material (five-parameter
172 Mooney-Rivlin model) with coefficients $C_{10} = 0.085$, $C_{01} = -0.058$, $C_{20} = 0.039$, $C_{11} = -0.023$, $C_{02} =$
173 0.009 , $D_1 = 3.652$, and $D_2 = 0$ MPa (Lemmon et al., 1997), are the most common material properties
174 used in the literature to model the EST. By comparing the stress-strain curves of these three materials
175 (Figure 5), the elastic behavior of the reported hyperelastic material was found to be very similar to that
176 of the linear elastic material with a modulus of 0.3 MPa, but very different from that of the linear elastic
177 material with a modulus of 1.15 MPa.

178



179

180 **Figure 5.** The stress-strain curves of three different material properties commonly used to model the

181

EST

182

183 To determine which reported elastic modulus is optimal for modeling the EST, we used our finite
184 element model of the foot to measure the ratio of unloaded heel pad thickness (UHPT) to loaded heel
185 pad thickness (LHPT) for each of these three material properties. In simulated plantar soft tissue with
186 hyperelastic material and linear elastic material with an elastic modulus of 0.3 MPa, the ratio of UHPT
187 to LHPT was 1.92 and 1.87, respectively, while the ratio in simulated plantar soft tissue with linear
188 elastic material with an elastic modulus of 1.15 MPa was 1.27 (Supplementary Table S1). When
189 compared to the ratio of 1.85 reported in a large population observational study (Ozdemir et al., 2004), it
190 was found that the hyperelastic material and the linear elastic material with an elastic modulus of 0.3
191 MPa can better simulate the material of the plantar soft tissue than the linear elastic material with an
192 elastic modulus of 1.15 MPa. Moreover, the foot modeled with EST with an elastic modulus of 1.15
193 MPa had significantly lower joint contact areas and pressures than the foot modeled with EST with an
194 elastic modulus of 0.3 MPa (Supplementary Table S2) or the reported hyperelastic material (Lakin et al.,
195 2001; Beaudoin et al., 1991; Kimizuka et al., 1980). This is due to the abnormally high stiffness of the
196 EST with an elastic modulus of 1.15 MPa, which prevented the cartilage from naturally contacting each
197 other.

198 To model the EST, both the reported hyperelastic material and linear elastic material with an elastic
199 modulus of 0.3 MPa can be used. However, a hyperelastic constitutive model more closely resembles
200 the inherent anisotropic and nonlinear behavior of the EST.

201

202 **2.2.4. Simulation of ligament failure**

203 Ligament tears or damage can occur from trauma, overuse, or degenerative disease. Because of their
204 poor blood supply, damaged ligaments may degenerate over time, resulting in overstretched and
205 elongated ligaments that lose their ability to function as foot stabilizers (Parvizi and Kim, 2010; Bray,
206 1995; Hauser et al., 2011; Fenwick et al., 2002). Ligaments can also creep, that is progressively elongate

207 due to a constant or cyclically repeated load (Frank, 2004). Either of these loading conditions can lead to
208 degenerative deformities such as progressive collapsing foot deformity (PCFD), also known as adult
209 acquired flatfoot (Johnson, 1983; Myerson et al., 2020).

210 In some cadaveric and computational studies, ligaments have been released to simulate ligament
211 failure and PCFD (Chu et al., 2001; Deland et al., 1992). In some cadaveric studies, ligaments become
212 elongated under high cyclic axial loading (Campbell et al., 2014; Dumontier et al., 2005). When
213 ligaments are progressively stretched to specific lengths, the loads within the ligament are significantly
214 reduced (Frank, 2004). In other words, ligament tears or elongation cause ligaments to be nonfunctional
215 because they bear no or little tension under normal working conditions. This is the same as having no
216 ligaments or having ligaments with no stiffness. Therefore, the absence of ligaments or pre-stretching
217 them to specific lengths properly simulates their failure to function as foot stabilizers.

218 On the other hand, some computational studies have reduced the stiffness of ligaments by half or
219 other fractions to simulate ligament failure and PCFD. Although a reduction in stiffness might be
220 observed in degenerated ligaments due to changes in their properties and geometry (Deland et al., 2005),
221 reducing ligament stiffness alone cannot reflect ligament failure. It is because the ligaments with
222 reduced stiffness are still tight and consequently functional.

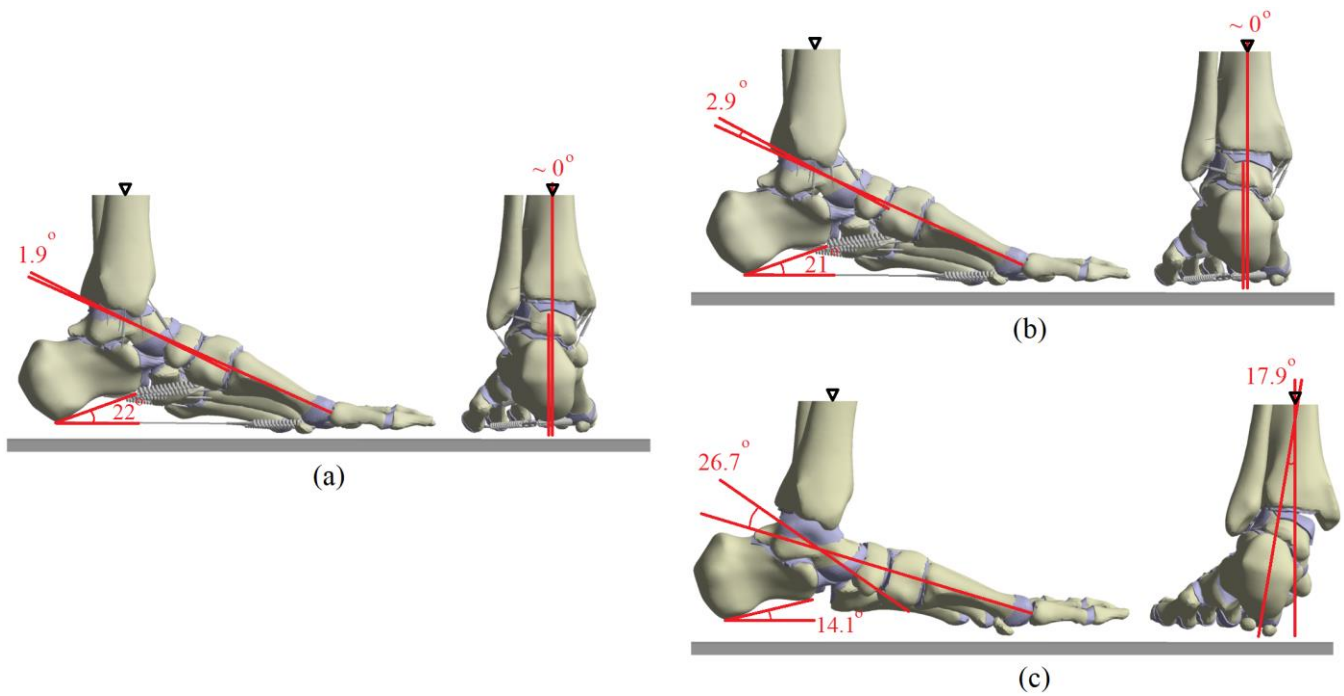
223 To clarify why reducing ligament stiffness cannot lead to PCFD (i.e., significant changes in foot
224 alignment and arch stability), we examine the stretch of the spring ligament under working conditions
225 when its stiffness is reduced by half. Reducing the stiffness of the spring ligament by half results in a
226 stretch of $x = 0.86 \text{ mm}$ ($F = kx \rightarrow x = F/k = 30 / (70/2) = 0.86 \text{ mm}$). However, PCFD is usually
227 associated with a tear in the spring ligament or nearly 10 mm degenerative elongation over time
228 (Malakoutikhah et al., 2022a). The stiffness ($k = 70 \text{ N/mm}$) and force values ($F = 30 \text{ N}$) for a normal
229 spring ligament were derived from the literature (Siegler et al., 1988; Malakoutikhah et al., 2022a).
230 These results are representative of relatively stiff ligaments even when their stiffness is reduced by half.

231 Due to the high stiffness, ligaments are subjected to a small amount of elastic strain under conditions of
232 normal physiologic loading (Robi et al., 2013; Maganaris and Narici, 2005).

233 We also used our finite element model of the foot to compare the foot alignment changes in a
234 collapsed foot simulated by reducing the stiffness of the ligaments by half versus removing the
235 ligaments (or pre-stretching them to specific lengths). The hindfoot alignment angle (HAA), calcaneal
236 pitch angle (CPA), and Meary's angle (MA) were used to evaluate the change in foot alignment
237 (Supplementary Figure 1S). Hindfoot valgus was assessed using the HAA, and arch collapse was
238 evaluated with both the MA and CPA. The clinical ranges of these angles reported for both normal foot
239 and collapsed foot are described in Supplementary Figure 1S.

240 Our results showed that all of the foot alignment angles were within the reported PCFD ranges in the
241 absence of ligaments (Figure 6c), but none were within the PCFD ranges in the case with reduced
242 stiffness ligaments (Figure 6b). The latter also failed to meet the criterion for a successful collapsed foot
243 model, which is defined as a 10° change in the MA (Campbell et al., 2014). This criterion was met when
244 the ligament stiffness was reduced by almost ten times (90%). This is also true for other deformities
245 such as hallux valgus, as a recent study on the sensitivity test on the ligaments showed that a minimum
246 of 80% reduction in ligament stiffness was needed to simulate a mild deformity (Wong et al., 2020).
247 Furthermore, the ligaments with reduced stiffness by half were subjected to about the same amount of
248 force as normal (naturally tight) ligaments bear in a normal foot. However, in real life, lax ligaments
249 bear only minor loads in PCFD (Frank, 2004). This unrealistic force in the ligaments with reduced
250 stiffness has the potential to alter the force pattern between joints and ligaments.

251



252

253 **Figure 6.** Foot alignment angles: a) in a normal foot simulated by keeping the ligaments and tendons

254 intact; b) in a collapsed foot simulated by reducing the stiffness of the ligaments by half; c) in a

255 collapsed foot simulated by removing the ligaments

256

257 **2.3. Loading and boundary conditions**

258 **2.3.1. Boundary conditions of the tibia**

259 Distal tibia motion in 3D space can be fully described by three translations (superior/ inferior, medial/

260 lateral, and anterior/ posterior) and three rotations (internal/ external, flexion/ extension, and varus/

261 valgus). In order to maintain ankle joint congruity, the rotation of the tibia must follow the talar dome

262 which is rotated externally or internally as the subtalar joint goes into varus or valgus due to the

263 orientation of the subtalar joint relative to the long axis of the foot (Inman's axis). Thus, the tibia is

264 rotated externally in pes cavus (high arched foot) and internally in pes planus (PCFD).

265 Most cadaveric and computational models have overlooked the need for tibial rotation and have fixed

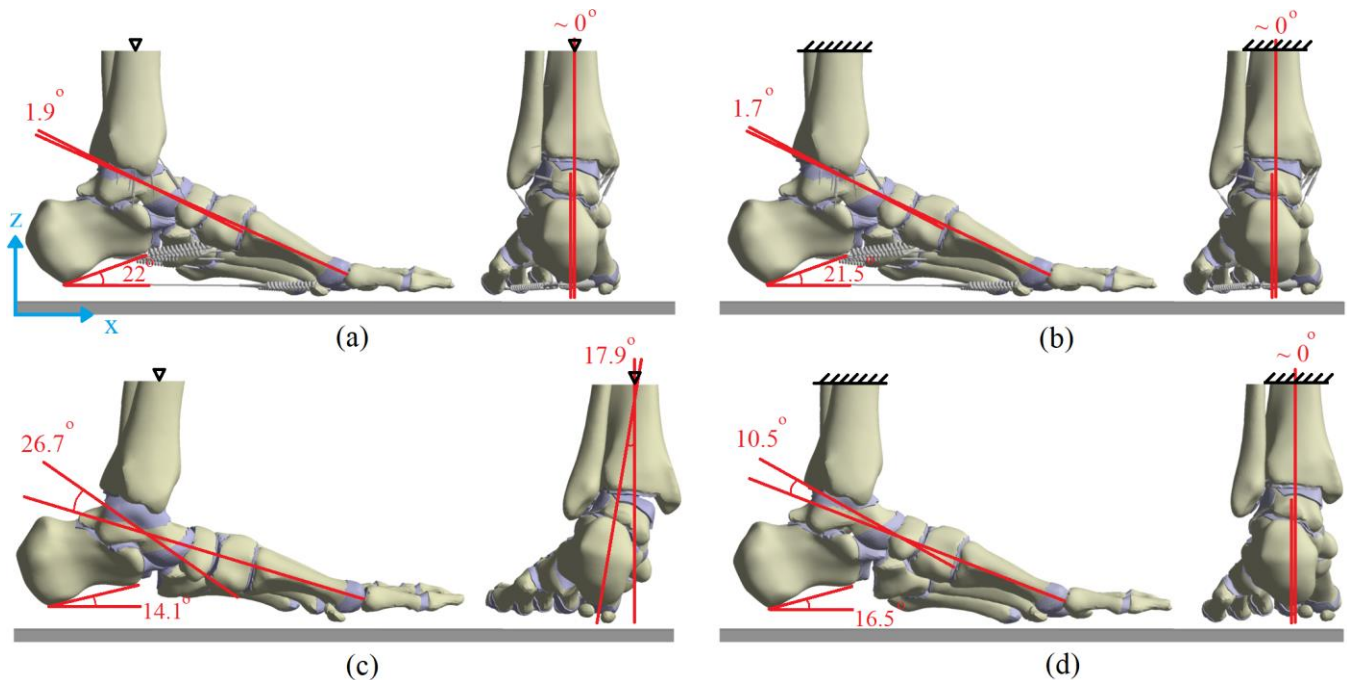
266 the tibia in all directions. While this may only lead to small errors in the study of a normally aligned

267 foot, we hypothesized that it might cause significant errors when studying disorders involving foot

268 malalignment (such as PCFD). To assess this, both normal foot and collapsed foot models were
269 examined in two different scenarios: (1) with the tibia fixed in all directions; and (2) with the tibia fixed
270 only in the z- direction (vertical) and allowed to translate in the x- and y-directions and rotate about all
271 three axes. In all cases, half the BW was applied to the ground, simulating ground reaction force.

272 We observed that the alignment angles of the normal foot with the tibia fixed in all directions (Figure
273 7b) were similar to those of the normal foot with the tibia free to move (Figure 7a). This similarity in the
274 results, which is due to the presence of ligaments and tendons as primary stabilizers of the foot, suggests
275 that fixing the tibia in all directions has no effect on foot alignment if the experiment is carried out on a
276 normal foot. On the other hand, the alignment angles of the collapsed foot with the tibia free to move
277 (Figure 7c) were all within the reported PCFD ranges, whereas the PCFD alignment angles with the tibia
278 fixed in all directions (Figure 8d) barely represented a mild PCFD. This is particularly true for the
279 hindfoot alignment angle (HAA), where fixing the tibia in all directions prevented valgus deformity of
280 the hindfoot. In conclusion, it is critical to allow the tibia to translate and rotate naturally in order to
281 simulate PCFD or any soft tissue transections.

282



283

284 **Figure 7.** Foot alignment angles in the simulated normal foot: a) with the tibia fixed only in vertical
285 direction, b) with the tibia fixed in all directions; Foot alignment angles in the simulated collapsed foot:
286 c) with the tibia fixed only in vertical direction, d) with the tibia fixed in all directions
287

288 **2.3.2. Loading conditions of the tibia**

289 The BW is carried by the tibia and transferred to the foot during standing and ambulation. In some
290 cadaveric and computational studies, half of the BW is applied upwards to the ground as the ground
291 reaction force, and the proximal tibia and fibula are fixed to simulate quiet stance. In other studies, the
292 ground is fixed, and half of the BW is applied downwards on the proximal tibia and fibula. However,
293 due to the action of muscles and their tendons, the total force in the tibia and fibula is usually greater
294 than the ground reaction force (0.5 BW). In particular, the Achilles tendon force, which is nearly a
295 quarter of the BW (Salathe and Arangio, 2002; Zhang and Fan, 2014), causes the forces applied in the
296 tibia and fibula to be nearly 1.5 times the ground reaction force (0.75 BW) during quiet stance. This can
297 be simply determined by the equilibrium condition for forces in the z-direction (Figure 8). Tendon
298 forces used to calculate the force in the tibia and fibula were obtained from the literature (Salathe and
299 Arangio, 2002; Morales-Orcajo et al., 2017). It must be noted that 93% of the applied load is transmitted
300 through the tibia and 7% through the fibula (Goh et al., 1992). Similarly, extremely high tendon forces
301 during walking and running (Giddings et al., 2000) result in greater forces in the tibia and fibula than the
302 ground reaction force. Due to the high value of the forces, even a small error in calculating their value
303 can cause significant changes in the results, especially when absolute values are reported.

304 Although forces can be applied to either the tibia or the ground, the ground is usually preferred
305 because the exact value of the ground reaction force can be measured with a scale and is not affected by
306 tendon forces.

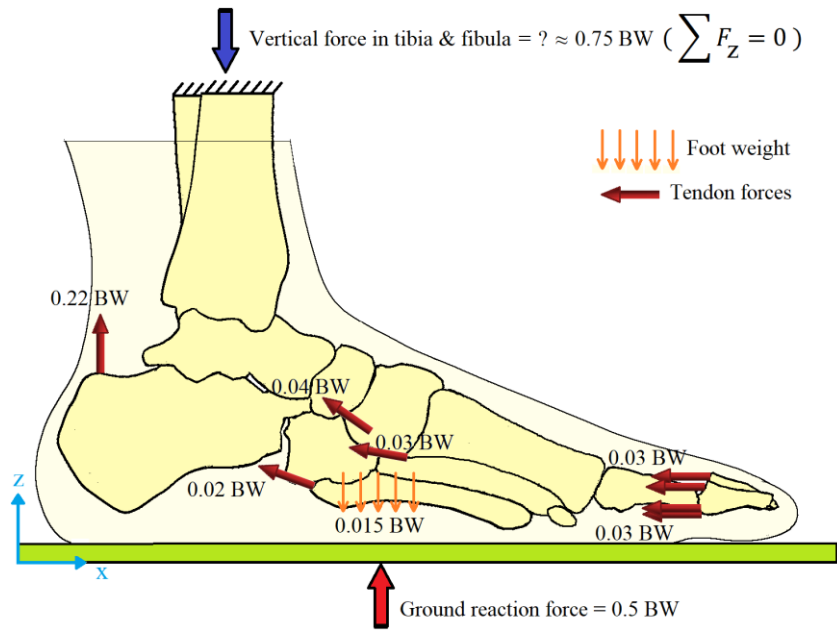


Figure 8. Free body diagram of the foot during simulated quiet stance

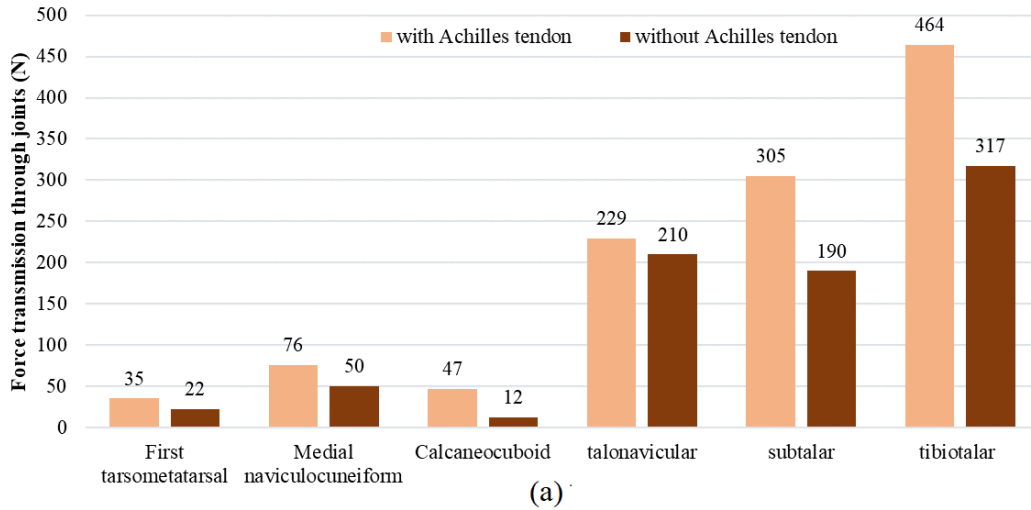
2.3.3. Neglecting the Achilles tendon force

Triceps surae muscle force is transferred through the Achilles tendon to the calcaneus, and from the calcaneus to the plantar fascia, and then to the metatarsal heads and the toes which exert force on the ground (Farris et al., 2020). Although most tendon forces have been ignored in computational modeling of the foot and ankle, because of the minimal reactions of intrinsic and extrinsic muscles during quiet stance (Basmajian and Stecko, 1963; Zhang and Fan, 2014), only a few have neglected the Achilles force. In contrast, many cadaveric models have not included tendon forces because of the difficulty of applying tendon forces in experimental setups.

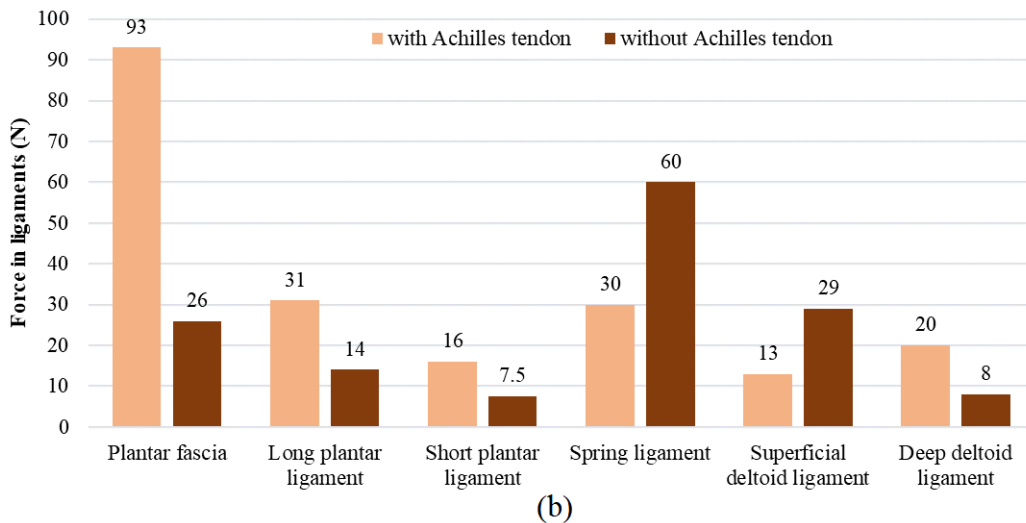
We hypothesized that neglecting the Achilles tendon force during cadaveric modeling would alter the pattern of force transmission throughout the foot. We used our foot model to simulate quiet stance both with and without the Achilles tendon force to examine how this simplification affects kinetic outcomes, including the force transmitted through the joints, force in the ligaments, and plantar pressure. We found that the force transmitted through all the joints decreased when the Achilles tendon force was removed

323 (Figure 9a). Moreover, removing the Achilles tendon significantly decreased the force within the plantar
 324 ligaments (plantar fascia, long plantar, and short plantar ligaments) and deep deltoid ligament, while it
 325 increased the force within the spring and superficial deltoid ligaments (Figure 9b). Our results of force
 326 in the plantar fascia are consistent with those obtained using an equation derived from a linear regression
 327 analysis (Erdemir et al., 2004). Moreover, the maximum plantar pressure in the heel fat pad increased
 328 from 164 kPa to 231 kPa when the Achilles tendon was removed (Figure 10). These varying changes in
 329 the force and pressure through the foot suggest that ignoring the Achilles tendon force can lead to
 330 significant errors.

331

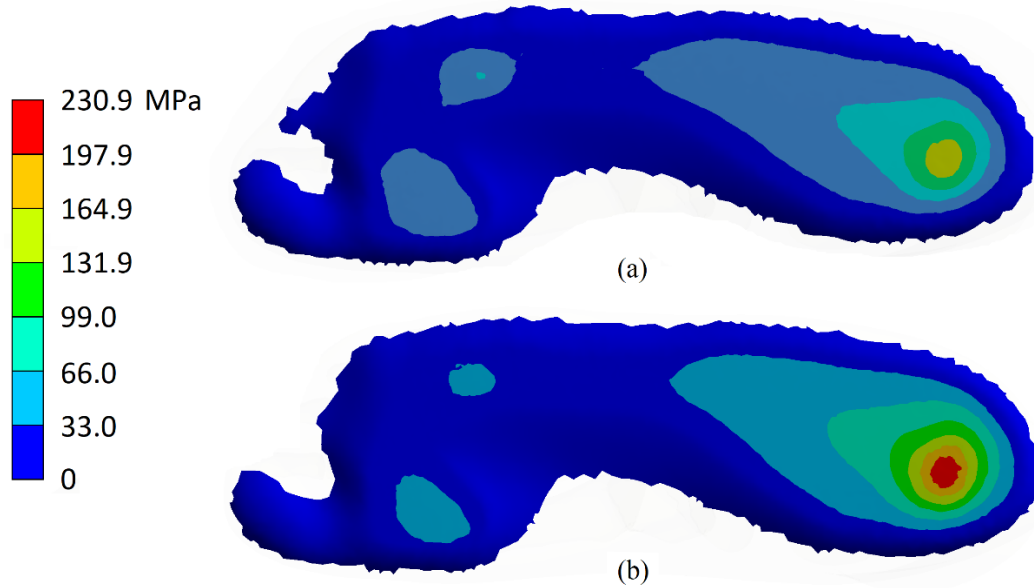


332



333

334 **Figure 9.** Comparison of the force (a) transmitted through the joints, and (b) within the ligaments,
335 between the foot with and without the Achilles tendon
336



337
338 **Figure 10.** Plantar pressure in the foot model (a) with the Achilles tendon, (b) without the Achilles
339 tendon
340

341 3. SUMARRY

342 We examined a number of the approaches used and the assumptions made in the development of
343 biomechanical models of the foot and ankle. We found that some assumptions made in defining
344 modeling parameters (element types, material properties, and loading and boundary conditions) led to
345 reduced accuracy or limited generalizability of their predictions.

346 The estimation of the element types and material properties is a key step in the creation of a
347 biomechanical model. A common source of error in modeling tendons and ligaments is the use of
348 isotropic solid elements, which allows them to transmit unrealistic bending/ twisting moments and
349 compressive forces rather than properly simulating their tension-only characteristics. Another source of
350 error associated with ligaments is the failure to assign proper stiffness values to ligaments with multiple

351 bands (e.g., the plantar fascia and the long plantar ligament). Because the bands are connected in
352 parallel, the stiffness of each band should be a percentage of the overall stiffness of these ligaments.
353 Ignoring the difference in elastic modulus between cortical and trabecular bones is the most common
354 assumption that affects stress distribution in the bones. In the case of the EST, the abnormally high
355 stiffness used in some computational models of the foot limits the normal deformation of the fat pad and
356 prevents the bones from naturally contacting each other.

357 A second key parameter is the boundary conditions. The proper selection of boundary conditions is
358 most important when there is abnormal motion of certain bones, for example in PCFD. It is necessary to
359 allow the tibia to rotate and translate in PCFD studies that involve ligament failure or tendon
360 dysfunction. We showed that fixing the tibia in all directions prevented hindfoot valgus deformity and
361 limited longitudinal arch collapse. Another essential factor in simulating ligament failure in PCFD is the
362 removal or pre-stretching of ligaments to specific lengths. We showed that reducing ligament stiffness
363 by percentages is unrealistic and insufficient to simulate ligament failure when producing PCFD. Our
364 findings may explain why previous studies that simulated PCFD by reducing ligament stiffness or fixing
365 the tibia in all directions only found a little to no malalignment.

366 Tendon forces and BW are the common loads that naturally apply to the foot under working
367 conditions. The total load that is transferred to the foot can be applied either downwards on the proximal
368 tibia and fibula or upwards to the ground while the other side is fixed. However, the amount of force in
369 the tibia and fibula is usually greater than the ground reaction force due to the presence of tendon forces.
370 The Achilles tendon has a relatively high force among all tendon forces. Neglecting the Achilles tendon
371 force can affect almost all kinetic and kinematic parameters through the foot. Specifically, it shifted the
372 tension from the plantar ligaments, particularly the plantar fascia, to the spring ligament, resulting in
373 significant changes in joint contact mechanics.

374 Although modeling a structure with the inherent complexity of the foot and ankle requires making
375 numerous simplifications, maintaining a few key reasonable modeling assumptions will help to produce
376 models with more realistic predictions.

377 One of the significant limitations of this study is that we only examined a few modeling assumptions.
378 The model used in this study to compare the results of various assumptions also has a number of
379 limitations, such as the use of linear elastic elements to model ligaments; the single-subject approach,
380 which limited the external validity of our findings (Wong et al., 2021); the use of a morphologically
381 normal foot to model the collapsed foot; and the use of non-weight-bearing CT scan, which required
382 determining the geometry and insertion points of the ligaments from the literature (Malakoutikhah et al.,
383 2022b).

384

385 **REFERENCES**

- 386 Akrami M, Qian Z, Zou Z, Howard D, Nester CJ, Ren L. Subject-specific finite element modelling of
387 the human foot complex during walking: sensitivity analysis of material properties, boundary and
388 loading conditions. *Biomech Model Mechanobiol.* 2018;17(2):559-576.
- 389 Altai Z, Qasim M, Li X, Viceconti M. The effect of boundary and loading conditions on patient
390 classification using finite element predicted risk of fracture. *Clin Biomech.* 2019;68:137-143.
- 391 Basmajian JV, Stecko G. The role of muscles in arch support of the foot, *J Bone Joint Surg Am.*
392 1963;45(6):1184-1190.
- 393 Beaudoin AJ, Fiore SM, Krause WR, Adelaar RS. Effect of isolated talocalcaneal fusion on contact in
394 the ankle and talonavicular joints. *Foot & ankle.* 1991;12(1):19-25.
- 395 Behforootan S, Chatzistergos P, Naemi R, Chockalingam N. Finite element modelling of the foot for
396 clinical application: A systematic review. *Med Eng Phys.* 2017;39:1-11.

397 Benjamin M, Ralphs JR. Fibrocartilage in tendons and ligaments--an adaptation to compressive load. J
398 Anat. 1998;193(Pt 4):481-494.

399 Bray R. Blood supply of ligaments: a brief overview. Orthopaedics. 1995;3:39-48.

400 Campbell ST, Reese KA, Ross SD, McGarry MH, Leba TB, Lee TQ. Effect of graft shape in lateral
401 column lengthening on tarsal bone position and subtalar and talonavicular contact pressure in a
402 cadaveric flatfoot model. Foot Ankle Int. 2014;35(11):1200-1208.

403 Chu I-T, Myerson MS, Nyska M, Parks BG, 2001. Experimental flatfoot model: the contribution of
404 dynamic loading. Foot Ankle Int. 2001;22(3):220-225.

405 Chu TM., Reddy NP, Padovan J. Three-dimensional finite element stress analysis of the polypropylene,
406 ankle-foot orthosis: static analysis. Med Eng Phys. 1995;17(5):372-379.

407 Cifuentes-De la Portilla C, Larrainzar-Garijo R, Bayod J. Biomechanical stress analysis of the main soft
408 tissues associated with the development of adult acquired flatfoot deformity. Clin Biomech.
409 2019;61:163-171.

410 Deland JT, de Asla RJ, Sung IH, Ernberg LA, Potter HG. Posterior tibial tendon insufficiency: which
411 ligaments are involved. Foot Ankle int. 2005;26(6):427-435.

412 Deland JT, Arnoczky SP, Thompson FM. Adult acquired flatfoot deformity at the talonavicular joint:
413 reconstruction of the spring ligament in an in vitro model. Foot Ankle Int. 1992;13(6):327-332.

414 Dumontier TA, Falicov A, Mosca V, Sangeorzan B. Calcaneal lengthening: investigation of deformity
415 correction in a cadaver flatfoot model. Foot Ankle Int. 2005;26(2):166-170.

416 Erdemir A, Hamel AJ, Fauth AR, Piazza SJ, Sharkey NA. Dynamic loading of the plantar aponeurosis
417 in walking. J Bone Joint Surg Am. 2004 Mar;86(3):546-52.

418 Farris DJ, Birch J, Kelly L. Foot stiffening during the push-off phase of human walking is linked to
419 active muscle contraction, and not the windlass mechanism. J. R. Soc. Interface. 2020;17(168)
420 172020020820200208.

421 Fenwick SA, Hazleman BL, Riley GP. The vasculature and its role in the damaged and healing tendon.
422 Arthritis Res. 2002;4(4):252-260.

423 Flores DV, Mejía Gómez C, Fernández Hernando M, Davis MA, Pathria MN. Adult acquired flatfoot
424 deformity: anatomy, biomechanics, staging, and imaging findings. Radiographics. 2019;39(5): 1437-
425 1460.

426 Frank CB. Ligament structure, physiology and function. J Musculoskelet Neuronal Interact.
427 2004;4(2):199-201.

428 Giddings V, Beaupr G, Whalen R, Carter D. Calcaneal loading during walking and running. Med Sci
429 Sports Exerc. 2000;32(3):627-634.

430 Goh JC, Mech AM, Lee EH, Ang EJ, Bayon P, Pho RW. Biomechanical study on the load-bearing
431 characteristics of the fibula and the effects of fibular resection. Clin Orthop Relat Res. 1992;279:223-
432 228.

433 Hao Z, Wan C, Gao X, Ji T. The effect of boundary condition on the biomechanics of a human pelvic
434 joint under an axial compressive load: a three-dimensional finite element model. J Biomech Eng.
435 2011;133(10):101006.

436 Hauser RA, Erin E, Dolan RN. Ligament injury and healing: An overview of current clinical concepts.
437 Journal of Prolotherapy. 2011;3(4):836-846.

438 Henry JK, Shakked R, Ellis SJ. Adult-acquired flatfoot deformity. Foot Ankle Orthop. 2019;4(1):1-17.

439 Hentges MJ, Gesheff MG, Lamm BM. Realignment subtalar joint arthrodesis. J Foot Ankle Surg.
440 2016;55(1):16-21.

441 Hsu CC, Tsai WC, Chen CP, Shau YW, Wang CL, Chen MJ, Chang KJ. Effects of aging on the plantar
442 soft tissue properties under the metatarsal heads at different impact velocities. Ultrasound in medicine
443 & biology. 2005;31(10):1423-1429.

444 Hu P, Wu T, Wang HZ, Qi XZ, Yao J, Cheng XD, Chen W, Zhang YZ. Influence of different boundary
445 conditions in finite element analysis on pelvic biomechanical load transmission. *Orthop Surg.*
446 2017;9(1):115-122.

447 Johnson KA. Tibialis posterior tendon rupture, *Clin. Orthop. Relat. Res.* 1983;177:140-147.

448 Kimizuka M, Kurosawa H, Fukubayashi T. 1980. Load-bearing pattern of the ankle joint. Contact area
449 and pressure distribution. *Arch Orthop Trauma Surg.* 1980;96(1):45-49.

450 Kitaoka HB, Luo ZP, Growney ES, Berglund LJ, An K-N. Material properties of the plantar
451 aponeurosis. *Foot Ankle Int.* 1994;15(10):557-560.

452 Lakin RC, DeGnore LT, Pienkowski D. Contact mechanics of normal tarsometatarsal joints. *J Bone*
453 *Joint Surg Am.* 2001;83(4):520-528.

454 Lemmon D, Shiang TY, Hashmi A, Ulbrecht JS, Cavanagh PR. The effect of insoles in therapeutic
455 footwear--a finite element approach. *J. Biomech.* 1997;30(6):615-620.

456 Maganaris CN, Narici MV. Mechanical properties of tendons. In: Maffulli N, Renström P, Leadbetter
457 WB, editors. *Tendon injuries: basic science and clinical medicine.* London: Springer London; 2005.
458 p. 14-21.

459 Malakoutikhah H, Madenci E, Latt LD. The contribution of the ligaments in progressive collapsing foot
460 deformity: a comprehensive computational study. *J. Orthop. Res.* 2022a;1-13.

461 Malakoutikhah H, Madenci E, Latt LD. A computational model of force within the ligaments and
462 tendons in progressive collapsing foot deformity. *J Orthop Res.* 2022b.

463 Morales-Orcajo E, Bayod J, Barbosa de Las Casas E. Computational foot modeling: scope and
464 applications. *Arch Computat Methods Eng.* 2016;23,389-416.

465 Morales-Orcajo E, Souza TR, Bayod J, Barbosa de Las Casas E. Non-linear finite element model to
466 assess the effect of tendon forces on the foot-ankle complex. *Med Eng Phys.* 2017;49:71-78.

467 Myerson MS, Thordarson DB, Johnson JE, Hintermann B, Sangeorzan BJ, Deland JT, Schon LC, Ellis
468 SJ, de Cesar Netto C. Classification and nomenclature: progressive collapsing foot deformity. *Foot*
469 *Ankle Int.* 2020;41(10):1271-1276.

470 Ozdemir H, Söyüncü Y, Ozgörgen M, Dabak K. Effects of changes in heel fat pad thickness and
471 elasticity on heel pain. *J Am Podiatr Med Assoc.* 2004;94(1):47-52.

472 Parvizi J, Kim GK, and Associate Editor. *High Yield Orthopaedics.* Saunders/ Elsevier, 2010; Chapter
473 88: pp.183-184.

474 Robi K, Jakob N, Matevz K, Matjaz V. The physiology of sports injuries and repair processes. *Current*
475 *Issues in Sports and Exercise Medicine*, edited by Michael Hamlin, Nick Draper, Yaso Kathiravel,
476 IntechOpen, 2013. 10.5772/54234.

477 Salathe EP, Arangio GA. A biomechanical model of the foot: the role of muscles, tendons, and
478 ligaments. *J. Biomech. Eng.* 2002;124(3):281-287.

479 Siegler S, Block J, Schneck CD. The mechanical characteristics of the collateral ligaments of the human
480 ankle joint. *Foot Ankle.* 1988;8:234-242.

481 Wang Y, Wong DW, Zhang M. Computational models of the foot and ankle for pathomechanics and
482 clinical applications: a review. *Ann Biomed Eng.* 2016;44(1):213-221.

483 Wong DW, Chen TL, Peng Y, Lam W, Wang Y, Ni M, Niu W, Zhang M. An instrument for
484 methodological quality assessment of single-subject finite element analysis used in computational
485 orthopaedics. *Med. Novel Technol. Dev.* 2021;11,100067.

486 Wong DW, Wang Y, Chen TL, Yan F, Peng Y, Tan Q, Ni M, Leung AK, Zhang M. Finite element
487 analysis of generalized ligament laxity on the deterioration of hallux valgus deformity (Bunion).
488 *Front Bioeng Biotechnol.* 2020;8,571192.

489 Zhang M, Fan Y. *Computational biomechanics of the musculoskeletal system.* 2014. CRC Press.